ISSN 1674-1056
http://cpb.iphy.ac.cn
http://iopscience.iop.org/cpb
中国物理 B
Chinese Physics
中国物理
Chinese Physics B

Robust stability characterizations of active metamaterials with non-Foster loads

Yi-Feng Fan(范逸风), Yong-Zhi Sun(孙永志)
Citation: Chin. Phys. B . 2018, 27(2): 028102. **doi:** 10.1088/1674-1056/27/2/028102

Journal homepage: http://cpb.iphy.ac.cn; http://iopscience.iop.org/cpb

What follows is a list of articles you may be interested in

Ultra-wideband circular-polarization converter with micro-split Jerusalem-cross metasurfaces

Xi Gao(高喜), Xing-Yang Yu(余行阳), Wei-Ping Cao(曹卫平), Yan-Nan Jiang(姜彦南), Xin-Hua Yu(于新华)
Chin. Phys. B . 2016, 25(12): 128102. **doi:** 10.1088/1674-1056/25/12/128102

Ultra-wideband reflective polarization converter based on anisotropic metasurface

Jia-Liang Wu(吴家梁), Bao-Qin Lin(林宝勤), Xin-Yu Da(达新宇)
Chin. Phys. B . 2016, 25(8): 088101. **doi:** 10.1088/1674-1056/25/8/088101

Polarization-insensitive unidirectional spoof surface plasmon polaritons coupling by gradient metasurface

Hong-yu Shi(施宏宇), An-xue Zhang(张安学), Jian-zhong Chen(陈建忠), Jia-fu Wang(王甲富), Song Xia(夏颂), Zhuo Xu(徐卓)
Chin. Phys. B . 2016, 25(7): 078105. **doi:** 10.1088/1674-1056/25/7/078105

All-dielectric frequency selective surface design based on dielectric resonator

Zheng-Bin Wang(王正斌), Chao Gao(高超), Bo Li(李波), Zhi-Hang Wu(吴知航), Hua-Mei Zhang(张华美), Ye-Rong Zhang (张业荣)
Chin. Phys. B . 2016, 25(6): 068101. **doi:** 10.1088/1674-1056/25/6/068101

Augmented Lyapunov approach to H_∞ state estimation of static neural networks with discrete and distributed time-varying delays

M. Syed Ali, R. Saravanakumar
Chin. Phys. B . 2015, 24(5): 050201. **doi:** 10.1088/1674-1056/24/5/050201

Robust stability characterizations of active metamaterials with non-Foster loads*

Yi-Feng Fan(范逸风)[1] and Yong-Zhi Sun(孙永志)[1,2,†]

[1] New Electromagnetic Materials Research Institute, Weifang University, Weifang 261061, China
[2] No. 8511 Research Institute of China, Aerospace Science Industry Corp., Nanjing 21007, China

(Received 11 July 2017; revised manuscript received 20 October 2017; published online 5 January 2018)

Active metamaterials incorporating with non-Foster elements have been considered as one of the means of overcoming inherent limitations of the passive counterparts, thus achieving broadband or gain metamaterials. However, realistic active metamaterials, especially non-Foster loaded medium, would face the challenge of the possibility of instability. Moreover, they normally appear to be time-variant and in unsteady states, which leads to the necessity of a stability method to cope with the stability issue considering the system model uncertainty. In this paper, we propose an immittance-based stability method to design a non-Foster loaded metamaterial ensuring robust stability. First, the principle of this stability method is introduced after comparing different stability criteria. Based on the equivalent system model, the stability characterization is used to give the design specifications to achieve an active metamaterial with robust stability. Finally, it is applied to the practical design of active metamaterial with non-Foster loaded loop arrays. By introducing the disturbance into the non-Foster circuit (NFC), the worst-case model uncertainty is considered during the design, and the reliability of our proposed method is verified. This method can also be applied to other realistic design of active metamaterials.

Keywords: active metamaterials, stability analysis, non-Foster circuit (NFC)

PACS: 81.05.Xj, 02.30.Yy **DOI:** 10.1088/1674-1056/27/2/028102

1. Introduction

Since Veselago introduced the concept of left-handed (LH) medium with simultaneous negative permittivity (ε) and permeability (μ),[1] the development of artificially engineered materials or metamaterials has been a subject of growing interest for both engineers and physicists due to their possible ability of designing and building novel devices.[2–4] It was shown that the realization of conventional metamaterials implies the use of the resonant structures,[5,6] which leads to the fact that the "negative" or "near-zero" material properties (ε and μ) are possible only within a narrow frequency band near the resonance, resulting in highly dispersive and lossy metamaterials. To overcome these limitations, a fair amount of attention has been paid to the design of novel metamaterials such as thermal metamaterials,[7] digital metamaterials,[8,9] and active metamaterials.[10,11] Particularly, active metamaterials by incorporating non-Foster circuits have attracted much attention due to their potential to break through the fundamental limits of passive metamaterials.[12,13]

To the best of our knowledge, the original idea of employing non-Foster elements to design the broadband metamaterials was theoretically proposed by Tretyakov.[10] However, the history of non-Foster antennas dates back to the 1930s when Bell lab applied the technique to reducing the size of relay coils in its early telephony systems.[14] Typically, non-Foster elements refer to negative lumped elements (i.e., negative capacitance, and negative inductance). Their reactance-versus-frequency slopes are negative, which are opposite to those of the ordinary positive lumped elements. Moreover, they are always realized by non-Foster circuits (NFCs). In Ref. [10], it was shown analytically that the loading of a short dipole with a negative capacitance would lead to the wideband non-dispersive ENG (ε-negative) behavior, meanwhile, the loading of a small loop with a negative inductance can lead to wideband dispersionless MNG (μ-negative) behavior. Although the subsequent theoretical study[15] illustrated the inherent instabilities of non-dispersive ENG and MNG metamaterials based on non-Foster elements, there had been a few studies about the realization of broadband MNG or MNZ (μ-near-zero) metamaterials with non-Foster loads,[11] in which both the stability and bandwidth enhancement were successfully achieved. Particularly, in Refs. [16] and [17], the Nyquist stability criterion was used to design an actively-loaded material which is capable of modeling the practical NFC circuits, including their parasitics and nonlinearities. Based on Cauchy's argument principle,[18] the product of the source impedance and load admittance forms a closed contour in the complex plane. By inspecting the encirclements of the point $(-1, 0)$, formed by the Nyquist contour, the stability of the system at a given operating point can be assessed.

In-depth investigation reveals that the Nyquist stability analysis also suffer some limitations. One drawback is that this

*Project supported by the National Natural Science Foundation of China (Grant No. 61701349), the Natural Science Foundation of Shandong Province, China (Grant Nos. ZR2017QF012 and ZR2017MF042), and the Program for the Top Young Innovative Talents, China (Grant No. Q1313-03).

†Corresponding author. E-mail: nanshen01@126.com

© 2018 Chinese Physical Society and IOP Publishing Ltd

technique cannot be used to formulate design specifications. Another drawback is that it can treat only a steady-state system. Some newly proposed stability methods for non-Foster loaded networks show the same problems.[19,20] However, for most electric systems, their performances are always limited by the system model uncertainty due to the perturbations, thus time-variant and unsteady-states appear. These perturbed objects include the parameter variation, steady-state error, time delay and noise. Thus, in the modern industry, to achieve a robust stability and keep the system stable up to the worst-case model uncertainty is a very important part of the design procedures. This also holds for active metamaterials, especially for non-Foster loaded metamaterials.

Due to these drawbacks mentioned above, in this paper we propose an immittance-based stability method, so as to break through these limitations, and achieve a non-Foster loaded active metamaterials while ensuring robust stability. This method can also be applied to the design of other active systems with non-Foster elements. After making a comparison between different stability criteria proposed in control theory, the principle of the immittance-based stability analysis is illustrated with respect to a closed-loop transfer function. With the specified gain boundary and phase boundary, the stability robustness of the system can be manipulated. Meanwhile, the original transfer function is modified in accordance with the cascaded source-load system we will use in this work. Subsequent to the application, an equivalent system model considering the system model uncertainty of a non-Foster loaded loop in a finite array is provided at first. Using the immittance-based stability characterization, the design specifications to achieve a stable non-Foster loaded active metamaterial are analytically derived which satisfy the specified robust stability conditions. These conditions are given by means of phase limitation and gain limitation as discussed in the principle illustration. Finally, the stability method is applied to the practical design of active metamaterials by physically realizing the non-Foster loads through using the resonant tunneling diode (RTD)-based NFC. The system model uncertainty is considered by introducing the disturbance into the RTD component. By inspecting the Nyquist curves of both disturbed and undisturbed models in the complex frequency plane, the robust stability of the system is verified. Furthermore, the effective parameters of the proposed active medium are extracted based on the system model of the single unit cell.

The rest of this paper is organized as follows. The principle of immittance-based stability analysis is introduced in Section 2. In Section 3, this stability characterization method is applied to the practical design of active metamaterial with non-Foster loads. Finally, some conclusions are drawn from the present study in Section 4.

2. Immittance-based stability analysis on a source-load system

So far, the stability analysis of time-varying networks has been extensively studied and lots of papers have derived various kinds of criteria for the stability problem.[21–32] Moreover, their principles are scalable and applicable to a wide range of active systems.Based on these principles, we may propose an immittance-based stability analysis method to analyze the stability of an active network with system uncertainty. For illustration, a cascaded source-load system is presented as shown in Fig. 1. There is a source with input impedance $Z_s(\theta_s,s)$ and a load with admittance $Y_l(\theta_l,s)$, where θ_s and θ_l are vectors of variables which determine all possible operating points of the source and load at the complex frequency $s(s=\sigma+\mathrm{j}\omega)$, respectively. The variance of the operating point is due to the perturbed objects leading to the model uncertainty of the system. Formally, the source impedance and load admittance are linearized transfer functions relating a change in voltage to a change in current at the terminals as follows:[25]

$$Z_s(\theta_s,s)=\left.\frac{\Delta v_s}{\Delta i_s}\right|_{X_s=\theta_s},\quad Y_l(\theta_l,s)=\left.\frac{\Delta i_l}{\Delta v_l}\right|_{X_l=\theta_l}. \tag{1}$$

Provided that the Nyquist plot of $Z_s(\theta_s,s)Y_l(\theta_l,s)$ of the source-load system at each operating point $\theta=[\theta_s\theta_l]$ does not encircle the -1 point in the complex frequency plane, we can say that this system has robust stability. This is a very important principle in the active system design, especially when a system includes non-Foster elements whose operating state normally appears to be time-variant and unsteady.

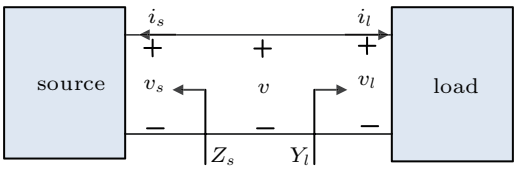


Fig. 1. Cascaded source-load system.

Another important application of the immittance-based stability analysis is that it can be used to formulate design specifications. That is, with the given source impedance (or load admittance), all possible operating points of the load admittance (or source impedance) can be obtained by keeping the Nyquist plots away from the forbidden region in the complex plane. This leads to a number of stability criteria, such as the opposing argument criterion,[21,22] Middlebrook criterion,[23] gain and phase margin (GMPM) criterion,[24] and the energy source analysis consortium (ESAC) criterion.[25,26] All these criteria determine various forbidden regions as shown in Fig. 2. Clearly, the ESAC criterion gives a least conservative design by constructing the smallest forbidden region, thus giving more allowable operating points. However, with a comprehensive review of these stability criteria,[27] we can observe that the ESAC criterion also suffers the limitation which

is not conducive to an easy design formulation. In contrast, the GMPM criterion is able to provide an analytic design specification to ensure the system stability, although it is more conservative.

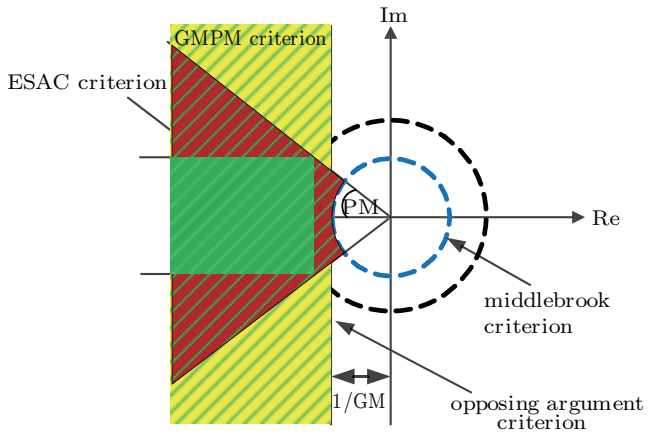


Fig. 2. (color online) Various stability criteria and their forbidden regions in the complex plane.[27]

A synthesization of the GMPM and ESAC criterion could lead to a more effective immittance-based stability analysis which has been proposed in Ref. [33]. We observe that this stability method is of potential significance for designing the active systems with non-Foster elements, although it is initially introduced for control system stability evaluation. Like the ESAC criterion, this stability method can also provide a less conservative forbidden region with the predefined conditions for robust stability. Moreover, it is able to formulate the design specifications serving as the GMPM criterion with the specified stability conditions.

For a control system with model uncertainty, its linear model can be expressed in the following form:[33]

$$y = Gu + G_{\mathrm{d}}d, \tag{2}$$

where y is the plant output, G is the plant model, G_{d} is the disturbance model, u is the plant input, and d is the disturbance. For a closed loop system, the plant model can be rewritten as

$$y = (1+L)^{-1}Lr + (1+L)^{-1}G_{\mathrm{d}}d - (1+L)^{-1}Ln, \tag{3}$$

where $L = GK$ is the loop transfer function, K is the controller, r denotes the reference value for the output, and n is the measurement noise. It has been proved that a closed-loop stability is dependent on the frequency response of the transfer function. As shown in Fig. 3, the principle of this stability method is illustrated by using a sample Nyquist plot $L(\mathrm{j}\omega)$ in the complex plane. Clearly, the system stability will be guaranteed if there are no encirclements of -1 point for the Nyquist curve. Furthermore, two stability parameters relating to the achievement of robust stability are indicated as well. One is the gain margin (GM), which is the reciprocal of the magnitude of the transfer function when the Nyquist curve first crosses the negative real-axis. The other is the phase margin (PM), which represents the phase of the function, when the Nyquist curve first crosses the unit circle. With the given gain boundary GM_s and phase boundary PM_s considering the worst-case model uncertainty, the design specifications to achieve a robust stable system can be formulated as

$$\mathrm{GM} = 1/|L(\mathrm{j}\omega_{180})| > \mathrm{GM}_s, \tag{4a}$$

$$\mathrm{PM} = 180 - \angle L_m(\mathrm{j}\omega_{\mathrm{c}}) > \mathrm{PM}_s, \tag{4b}$$

where

$$\angle L(\mathrm{j}\omega_{180}) = 180^{\circ}, \tag{5a}$$

$$|L(\mathrm{j}\omega_{\mathrm{c}})| = 1. \tag{5b}$$

It should be noted that with the bigger values of GM_s and PM_s increasing, the safeguard against the system error becomes stronger, although the design specifications will become more conservative.

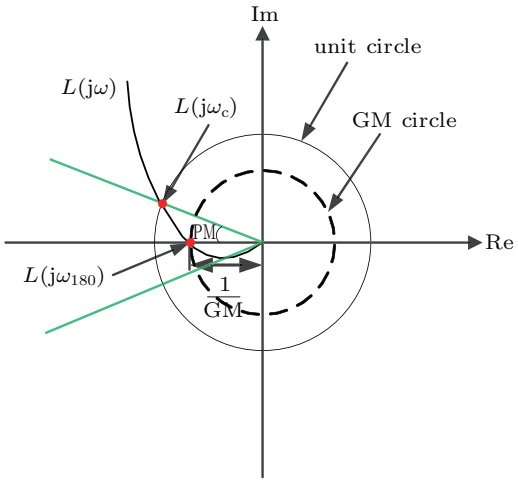


Fig. 3. (color online) Typical Nyquist plot of a closed loop transfer function for stable operating point indicated with PM and GM.[33]

For a cascaded source-load system as shown in Fig. 1, however, the plant model must be modified in accordance to the stability method. Here, the following plant-like model is given in the form of (see Ref. [33])

$$\begin{aligned} v &= \frac{N_l D_s v_s + N_s D_l v_l}{N_l D_s (1 + Z_s Y_l)} \\ &= (1 + Z_s Y_l)^{-1} Z_s Y_l (Z_l Y_s v_s + V_l), \end{aligned} \tag{6}$$

where

$$Z_s = \frac{N_s}{D_s}, \quad Z_l = \frac{N_l}{D_l} \tag{7}$$

are the source and load impedance in the form of fractions. By comparing Eq. (6) with Eq. (3), it is straightforward to derive the unsteady-state transfer function of a cascaded source-load system by using the following expression:

$$L(\theta, s) == Z_s(\theta_s, s) Y_l(\theta_l, s)\big|_{\theta=[\theta_s, \theta_l]}, \tag{8}$$

where the system model uncertainty has been taken into account by operating point vector $\theta = [\theta_s \theta_l]$. Therefore, the conditions to achieve the robust stability for the cascaded source-load system can be obtained by substituting Eq. (8) into Eqs. (4a) and (4b).

3. Applications in the design of active metamaterials

In this section, the proposed immittance-based stability method is employed to provide the design specifications of a practical non-Foster loaded active metamaterial while ensuring robust stability. First, the equivalent system model of the active metamaterials is presented. The analytic stability bounds of the non-Foster circuit based on the system model are then studied to make the unsteady-state system stable with the assumed model uncertainty. Finally, an experimental demonstration with practical NFC design is provided for validation.

3.1. Equivalent system model

In Ref. [11], it was suggested that periodic loops with non-Foster loads could be used to create a stable low-dispersion MNG or MNZ metamaterials, although in practice the choice of load would be restricted by the instability criterion.

At a radial frequency ω, the impedance of a loop m with an arbitrary load Z_L is,[34]

$$Z_m = \left[\frac{1}{R_m + \mathrm{j}\omega L_m} + \frac{\mathrm{j}\omega C_m}{1 + \mathrm{j}\omega C_m R_C}\right]^{-1} + Z_L, \tag{9}$$

where L_m is the self-inductance of the loop, R_m is the sum of the radiation resistance R_r and the Ohmic resistance R_w, and C_m is the loop capacitance which, despite contributing little to the effective materials' properties, cannot be ignored for stability analysis of the actively loaded medium. For the case of an array of identical loops, we henceforth define L_m, R_m, and C_m as L_0, R_0, and C_0 respectively.

An equivalent circuit of N loaded loops is shown in Fig. 4. Interactions between any two loops (m, n) in the system are represented by a mutual impedance $Z_{mn} = \mathrm{j}\omega M_{m,n}$ where $M_{m,n}$ represents the mutual inductance. So, a general relationship linking the currents and voltages of all loops can be obtained in the matrix form as follows:[34]

$$\left[(Z_0 + Z_L)\,\bar{\bar{E}} + \mathrm{j}\omega\bar{\bar{M}}\right]\bar{I} = \bar{V}, \tag{10}$$

where $\bar{\bar{E}}$ is the identity matrix, $\bar{I}$ and $\bar{V}$ are N-dimensional vectors

$$\bar{I} = (I_1, I_2, \ldots, I_N); \quad \bar{V} = (V_1, V_2, \ldots, V_N), \tag{11}$$

and

$$\bar{\bar{M}} = (M_{mn}) = \begin{cases} 0, & \text{if } m = n, \\ M_{|m-n|}, & \text{if } m \neq n \end{cases} \tag{12}$$

is a symmetrical $N \times N$ matrix representing the mutual couplings between different loops. By solving the characteristic polynomial of Eq. (2), the stability of the system can be determined by investigating the roots of the characteristic equation of each eigenvalue of the system matrix, that is,[11]

$$\lambda = Z_0(s) + Z_L(s) + s\lambda_m, \tag{13}$$

where $\lambda_m\,(m \in (1, \ldots, N))$ is the m-th eigenvalue of the mutual coupling matrix $\bar{\bar{M}}$. Therefore, the equivalent system model for the m-th loop can be obtained in the complex frequency domain during the immittance-based stability analysis. As a cascaded source-load system, it can be regarded as a series connection of the loop itself Z_0, the active load Z_L, and the equivalent mutual inductance λ_m. The $Z_L(s) = R_L||L_L||C_L$ is a parallel negative lumped-*RLC* network which is used to achieve stable broadband MNG or MNZ metamaterials,[16,17] although the stability analysis proposed in the literature is only for nominal stability without considering the model uncertainty of the practical system. Particularly, considering nearest-neighbor interactions only, which is enough for the accurate prediction of the phenomenon, the m-th eigenvalue can be solved, leading to the following expression:

$$\lambda_m = 2M\cos(m\pi/N + 1), \tag{14}$$

where M represents the mutual inductance between adjacent loops.

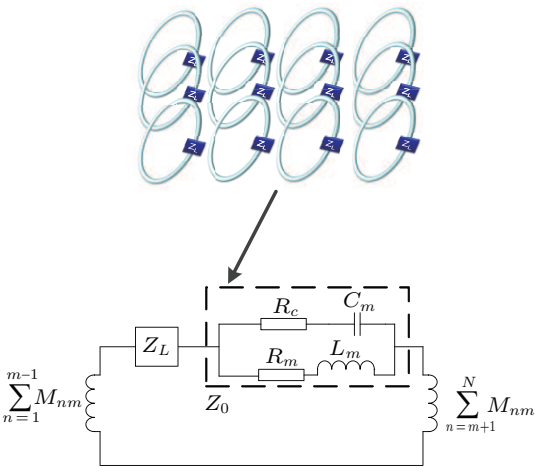


Fig. 4. (color online) Equivalent circuit of a loop and load in a system of N coupled loaded loops.[11] Summations indicate the coupling factors between the loop m and the remaining loops.

The determination of the source and load of the system, also named components grouping, are very important during the stability analysis by using Nyquist plots. From the Nyquist theory,[26] it is required that neither the source impedance or the load admittance have any pole in the RHP for the "open loop" case. Moreover, an open circuit stable (OCS) NIC which would be employed for this design has all impedance poles in the LHP,[35] thus has to be determined as a source. Clearly, a

passive loop would have all the impedance poles and zeros in the LHP, therefore satisfies the specifications of being a source or a load. From 4, it is straightforward that the NIC load Z_L must be stable for an open circuit state, thus should be defined as the system source. Meanwhile, the loop itself with the coupled inductance should be defined as the system load. Their impedance/admittance can be written as

$$Z_s(\theta_s,s) = Z_L(s)|_{X_s=\theta_s}, \tag{15a}$$

$$Y_l(\theta_l,s) = \left.\frac{1}{Z_0(s)+s\lambda_m}\right|_{X_l=\theta_l}. \tag{15b}$$

According to the immittance-based stability analysis for a cascaded source-load system as presented in Section 2, the frequency response of the m-th loop transfer function can be obtained based on the equivalent system model, that is,

$$L_m(s) = Z_s(\theta_s,s)Y_l(\theta_l,s) = \left.\frac{Z_L(s)}{Z_0(s)+s\lambda_m}\right|_{\theta=[\theta_s,\theta_l]}. \tag{16}$$

3.2. Stability characterization

As discussed before, to design an active system satisfying the conditions for robust stability, it is required that the Nyquist plots in the complex frequency domain avoid the forbidden region due to the model uncertainty. As proposed before, this region can be formulated by using the gain boundary and phase boundary. Since the loop capacitance C_0 and its cascade connected resistance R_C for an electrically small loop are usually very small, they can be ignored during the algebraic operations. So, the frequency response of the Nyquist plot of the m-th loop system can be obtained from Eq. (16) as follows:

$$L_m(\mathrm{j}\omega) = \frac{\mathrm{j}\omega R_L L_L}{(R_L-\omega^2 R_L L_L C_L+\mathrm{j}\omega L_L)(R_0+\mathrm{j}\omega L_0+\mathrm{j}\omega\lambda_m)}, \tag{17}$$

leading to the following expression for the phase and magnitude distributions

$$\angle L_m(\mathrm{j}\omega) = 90^\circ - \arctan\left(\frac{\omega L_L}{R_L-\omega^2 R_L L_L C_L}\right) - \arctan\left(\frac{\omega L_0+\omega\lambda_m}{R_0}\right), \tag{18a}$$

$$|L_m(\mathrm{j}\omega)| = \frac{\omega R_L L_L}{\sqrt{(R_L-\omega^2 R_L L_L C_L)^2+\omega^2 L_L^2}} \times \frac{1}{\sqrt{R_0^2+\omega^2(L_0+\lambda_m)^2}}. \tag{18b}$$

Upon the substitution of Eqs. (17) and (18a) in Eq. (4a), the stability condition with the given gain boundary GM_s guarding against steady-state error is satisfied, thus leading to the following analytic bounds for the non-Foster inductance:

$$0 > L_L > \approx -\frac{R_L(L_0+\lambda_m)}{\mathrm{GM}_s\cdot R_L+R_0}, \tag{19}$$

where R_L is a predefined negative resistance with the specification $|R_L| \ll R_0$. In a similar manner, the stability bounds for the non-Foster capacitance can be analytically derived by substituting Eqs. (17) and (18a) into Eq. (4b) as follows:

$$0 > C_L > \frac{(L_0+\lambda_m)(L_0+\lambda_m+L_L\cos(\mathrm{PM}_s))}{R_L^2 L_L \sin(\mathrm{PM}_s)^2}, \tag{20}$$

which satisfies the phase margin specification used as a safeguard against time delay uncertainty.

Comparing with the nominal stability analysis of a steady-state magneto-inductive metamaterial proposed in Refs. [16] and [17], it is clear to see that the range of stable values of non-Foster inductance will decrease if we assume $\mathrm{GM} > 1$. Furthermore, it appears that as the magnitude of non-Foster capacitance decreases, the Nyquist curve will deviate from the uncertain region with respect to the PM specifications in the complex plane, thus the system robustness will be enhanced. It should be noted that the stability condition described by using Eqs. (19) and (20) must hold for all λ_m values in a finite system. However, it is not difficult to observe that when the loop number increases and moves towards infinity ($N \to \infty$), the m-th eigenvalue λ_m can be replaced by a constant mutual inductance represented as M_p ($M_p \approx 2M$). This change can be applied to all loop models.

3.3. Application

In order to validate the above analysis, we shall now apply the proposed immittance-based stability method to the practical design of active metamaterials. The equivalent system model of a practical non-Foster loaded loop in an infinite active medium is presented as shown in Fig. 5. Figure 5 also gives the physical realization of the non-Foster load by using RTD-based NFC.[12] Therein, a π-type negative impedance inverter (NII) is employed to achieve the impedance transformation. It consists of a pair of passive resistors with the same value of R, and an RTD represented as a negative resistor with the opposite value. In contrast to the previously transistorized NFC design mostly based in Linvill's NIC circuit,[35] this NII circuit employs a cascaded RLC as the NFC input to achieve a parallel negative-RLC in the output terminal. It should be noted that the system uncertainty is considered here, by introducing a disturbance into the RTD component, that is,

$$d = \Delta_\mathrm{d} R, \tag{21}$$

where Δ_d is the normalized disturbance. Therefore, the output impedance of the NFC can be obtained to be

$$Z_L = R||(-R+\Delta_\mathrm{d}R+R||Z_N), \tag{22}$$

where Z_N is the series impedance of the lumped resistance R_N, inductance L_N, and capacitance C_N. Moreover, under the assumption of an undisturbed model ($\Delta_d = 0$), we may rewrite Eq. (22) in the form of a parallel lumped-RLC network with the following expressions

$$R_L = -\frac{R^2}{R_N}, \quad L_L = -C_N R^2, \quad C_L = -\frac{L_N}{R^2}. \tag{23}$$

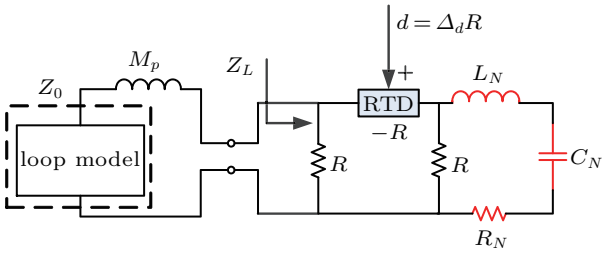


Fig. 5. (color online) Equivalent system model of a practical non-Foster loaded loop in an infinite active medium. The non-Foster load is realized by using the RTD-based NFC.

Assume that the practical active metamaterial design has the following parameters: each loop is made of copper with a conductivity of 5.8×10^7 S/m. The physical dimensions for each of the loops are represented by the loop radius $r_0 = 10$ mm and wire radius $r_w = 1$ mm. Thus, the self-impedance of each loop Z_0 can be theoretically obtained (see Ref. [34]). The active medium design is based on an infinite coaxial loop array with a 10-mm period. Assuming that the worst-model uncertainty of the RTD component is $\Delta_d = \pm 10\%$, we may determine the gain boundary and phase boundary of the system to be $GM_s = 2$, and $PM_s = 5^\circ$. The loop itself and other lumped elements each can be regarded as a time-invariant linear component, thus they can be ignored during the system error evaluation. Under the assumption of the non-Foster resistance $R_L = -1000\ \Omega$, the stability bounds for the non-Foster inductance can be found to be $0 > L_L > -21.5$ nH by using Eq. (19). Here, we choose $L_L = -18$ nH as the desired negative inductance. Substituting all these parameters into Eq. (20), we obtain a range of non-Foster capacitances $0 > C_L > -7.86$ pF, and then the negative capacitance is randomly chosen to be $C_L = -4.8$ pF. Ignoring the RTD disturbance, the input *RLC* values of the NFC can be obtained by using Eq. (23) through assuming the RTD resistance to be $-50\ \Omega$, that is, $R_N = 2.5\ \Omega$, $L_N = 12$ nH, and $C_N = 7.2$ pF.

Since we have obtained all circuit values of the system model already, it is straightforward to investigate the robust stability of the system by considering the RTD disturbance. As mentioned before, we consider two disturbed models in a worst case, respectively: model 1 with an RTD resistance of $-45\ \Omega$ arriving at a normalized disturbance of $+10\%$, and model 2 with the -10% disturbed RTD resistance of $-55\ \Omega$. The stability of the proposed medium is investigated in the complex frequency plane.

Figure 6 shows the Nyquist curves of the system with considering the worst-model uncertainty, for comparing with those from the undisturbed model. Moreover, we also plot the specified gain boundary and phase boundary to provide a visible insight into the stability robustness. By amplifying the region around the gain boundary and phase boundary as shown in Fig. 6(b), we can observe the differences between the disturbed models and the undisturbed model. The details of the stability parameters for different models are provided in the following Table 1. By comparing the Nyquist curves of different models, it is shown that none of these Nyquist curves including both the disturbed model 1 and model 2 and undisturbed model has any encirclement of -1 point, thus signifying the stability. Therefore, we can conclude that the system stability of our proposed active medium design can be guaranteed up to the worst-model uncertainty.

Table 1. Stability parameters of proposed active medium.

Symbols	Parameters	Undisturbed model	Disturbed model 1	Disturbed model 2
Δ_d/%	normalized RTD disturbance	0	-10	$+10$
$-R/\Omega$	RTD resistance	–50	–45	–55
GM	Gain margin	2.38	2.14	1.23
PM/(°)	Phase margin	6.53	22	3

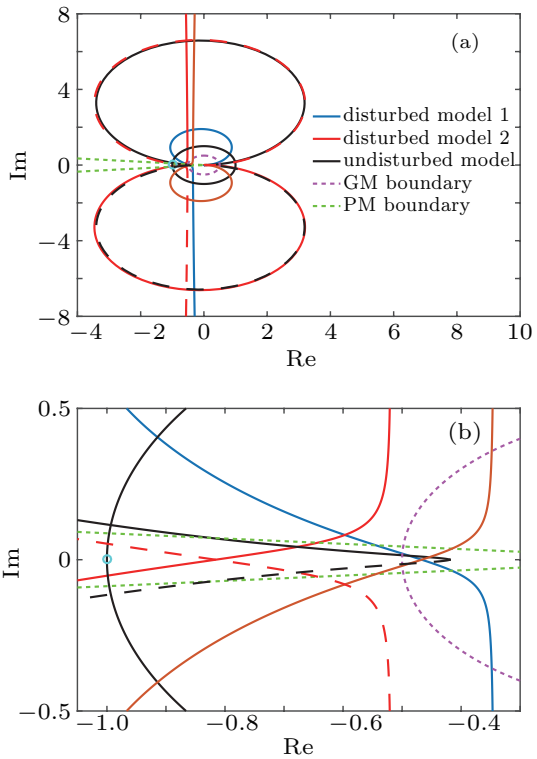


Fig. 6. (color online) (a) Nyquist contours of the proposed medium for the disturbed models, as compared with the result for the undisturbed model. (b) Magnified part of Nyquist contours around the -1 point. Disturbed model 1 (blue line) corresponds to the system with a normalized RTD disturbance of $+10\%$, while disturbed model 2 (red line) corresponds to the case of -10%.

Verifying the robust stability through examination, now we could use the analytic results to predict the effective parameters of a non-Foster loaded active metamaterial. According to the theory proposed in Ref. [11], the relative permeability of the active medium with respect to the equivalent system model can be expressed as follows:

$$\mu_{\mathrm{r}} = 1 - \mu_{\mathrm{b}} N \frac{\mathrm{j}\omega S^2}{Z_0 + Z_L + \mathrm{j}\omega M_p}, \tag{24}$$

where μ_{b} is the background permeability, S is the loop area, N is the volume density of loops. Upon the substitution of all parameters in Eq. (24), the frequency spectrum of the effective permeability of this active medium can be extracted as shown in Figs. 7. For comparison, both the disturbed models and the undisturbed model are considered here. Clearly, the disturbance of the RTD component has a great influence on the material properties of the active medium. As shown in Fig. 7(a), the disturbed model 1 shows a wideband MNZ behavior, while the disturbed model 2 presents a wideband MNG metamaterial. Figure 7(b) shows the curves for imaginary permeability versus frequency of the proposed medium. It is interesting to note that either the disturbed model 1 or the undisturbed model, presents a positive peak in the imaginary spectrum, while the disturbed model 2 shows the opposite behavior. According to Ref. [16], we can conclude that disturbed model 1 and the undisturbed model show a gain effect, while the disturbed model 2 shows loss effect.

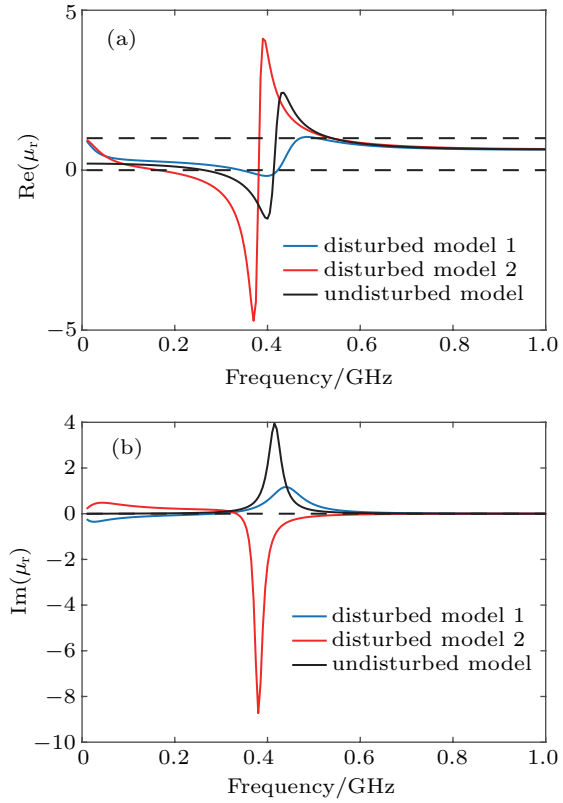


Fig. 7. (color online) Extracted effective permeability of the active medium for the disturbed models compared with the result for the undisturbed model. (a) Real part, (b) imaginary part.

4. Conclusions

An immittance-based stability method is proposed in order to practically design the active metamaterials with non-Foster loads ensuring robust stability. By making comparison between different stability criteria, a stability method synthesizing the merits of two existing stability criterion is introduced and modified in accordance to the cascaded source-load system. With the presented equivalent system model, this stability method is applied to the practical design of active metamaterials with non-Foster loaded loop arrays. According to the specifications of the gain margin and phase margin to satisfy the requirements for robust stability, we obtain the analytic bounds for the non-Foster elements. Subsequently, the fabricated and measured RTD-based NFC are demonstrated experimentally. The measurement results show the excellence of the NFC performance. The robust stability of a practical non-Foster loaded loop is checked in the complex plane, and the effective parameters of an infinite medium or a finite structure with a fair number of unit cells are further predicted.

References

[1] Veselago Viktor G 1968 *Soviet Physics Uspekhi* **10** 509
[2] Smith D R, Padilla W J, Vier D C, Nemat-Nasser S C and Schultz S 2000 *Phys. Rev. Lett.* **84** 4184
[3] Pendry J B 2000 *Phys. Rev. Lett.* **85** 3966
[4] Schurig D, Mock J J, Justice B J, Cummer S A, Pendry J B, Starr A F and Smith D R 2006 *Science* **314** 977
[5] Pendry J B, Holden A J, Robbins D J and Stewart W J 1999 *IEEE Trans. Microwave Theor. Techniq.* **47** 2075
[6] Ozbay E, Aydin K, Cubukcu E and Bayindir M 2003 *IEEE Trans. Anten. Propag.* **51** 2592
[7] Shen X Y, Huang J P 2016 *Acta Phys. Sin.* **65** 178103 (in Chinese)
[8] Cui T J, Qi M Q, Wan X and Zhao J 2014 *Light: Science & Applications* **3** e218
[9] Cui T J, Liu S and Li L L 2016 *Light: Science & Applications* **5** e16172
[10] Tretyakov S A 2001 *Microwave and Optical Technology Letters* **31** 163
[11] Rajab K Z, Hao Y, Bao D, Parini C G, Vazquez J and Philippakis M 2010 *J. Appl. Phys.* **108** 054904
[12] Nagarkoti D S, Hao Y, Steenson D P, Li L, Linfield E H and Rajab K Z 2016 *IEEE Anten. Wireless Propag. Lett.* **15** 1398
[13] Mou J, Shen Z 2017 *IEEE Trans. Anten. Propag.* **65** 696
[14] Crisson G 1931 *Bell Labs Technical Journal* **10** 485
[15] Tretyakov S A and Maslovski S I 2007 *IEEE Anten. Propag. Mag.* **49** 37
[16] Fan Y, Nagarkoti D S, Rajab K Z, Hao Y, Zhang H C and Cui T J 2016 *J. Appl. Phys.* **119** 194904
[17] Rajab K Z, Fan Y F and Hao Y 2012 *J. Opt.* **14** 114004
[18] Kreyszig E 2010 *Advanced engineering mathematics* (John Wiley & Sons)
[19] Tang Q and Xin H 2017 *IEEE Trans. Microwave Theor. Techniq.* **65** 3269
[20] Loncar J, Hrabar S and Muha D 2017 *IEEE Trans. Anten. Propag.* **65** 390
[21] Feng X, Ye Z, Xing K, Lee F C and Borojevic D 1999 *IEEE 30th Annual Power Electronics Specialists Conference* **2** 889
[22] Feng X, Liu J and Lee F C 2002 *IEEE Trans. Power Electron.* **17** 157
[23] Middlebrook R D 1976 *IAS'76*

[24] Wildrick C M, Lee F C, Cho B H and Choi B 1995 *IEEE Trans. Power Electron.* **10** 280
[25] Sudhoff S D and Glover S F 2000 *IEEE* 31*st Annual in Power Electronics Specialists Conference (PESC* 2000*)* **1** 101
[26] Sudhoff S D, Glover S F, Lamm P T, Schmucker D H and Delisle D E 2000 *IEEE Transactions on Aerospace and Electronic Systems* **36** 965
[27] Riccobono A and Santi E 2014 *IEEE Trans. Industry Appl.* **50** 3525
[28] Afzal S, Asghar S and Ahmad A 2017 *Chin. Phys. B* **26** 014704
[29] Liu C, Liu S X and Mei F X 2016 *Chin. Phys. B* **25** 124501
[30] Alqadi M K 2015 *Chin. Phys. B* **24** 118404
[31] Wang R, Sun Hui and Yang M Z 2015 *Chin. Phys. B* **24** 040201
[32] Wang J, Hui G T and Xie X P 2013 *Chin. Phys. B* **22** 030206
[33] Skogestad S and Postlethwaite I 2007 *Multivariable feedback control: analysis and design*, Vol. **2** (New York: Wiley) p. 458
[34] Tretyakov S A, Mariotte F, Simovski C R, Kharina T G and Heliot J P 1996 *IEEE Trans. Anten. Propag.* **44** 1006
[35] Linvill J 1953 *Proceedings of the IRE* **6** 725